

Structural Evidence for a Dominant Role of Nonpolar Interactions in the Binding of a Transport/Chemosensory Receptor to Its Highly Polar Ligands<sup>†,‡</sup>Xiaoqun Duan<sup>§</sup> and Florante A. Quijcho\**Howard Hughes Medical Institute and Department of Biochemistry and Molecular Biology, Baylor College of Medicine, Houston, Texas 77030**Received September 19, 2001*

**ABSTRACT:** The receptor, a maltose/maltooligosaccharide-binding protein, has been found to be an excellent system for the study of molecular recognition because its polar and nonpolar binding functions are segregated into two globular domains. The X-ray structures of the “closed” and “open” forms of the protein complexed with maltose and maltotetraol have been determined. These sugars have ~3 times more accessible polar surface (from OH groups) than nonpolar surface (from small clusters of sugar ring CH bonds). In the closed structures, the oligosaccharides are buried in the groove between the two domains of the protein and bound by extensive hydrogen bonding interactions of the OH groups with the polar residues confined mostly in one domain and by nonpolar interactions of the CH clusters with four aromatic residues lodged in the other domain. Substantial contacts between the sugar hydroxyls and aromatic residues are also formed. In the open structures, the oligosaccharides are bound almost exclusively in the domain rich in aromatic residues. This finding, along with the analysis of buried surface area due to complex formations in the open and closed structures, supports a major role for nonpolar interactions in initial ligand binding even when the ligands have significantly greater potential for highly specific polar interactions.

Molecular recognition between a protein and its ligand is the basis of biological and biochemical specificity and activity. Because recognition processes frequently involve both polar and nonpolar interactions, it is paramount to differentiate and experimentally assess the contribution of both types of interactions in these processes. Besides the distinct role of each domain of the maltose/maltooligosaccharide-binding protein (MBP),<sup>1</sup> the fact that the ligands are highly polar oligosaccharides further affords the system a particularly stringent, or possibly limiting, test of the importance of nonpolar interactions in molecular recognition and binding.

MBP (mass of 40 kDa) is a member of a superfamily of primary receptors for bacterial ABC-type active transport and chemotaxis (1–3). The crystal structure of MBP, like numerous other members of its superfamily (4), consists of two distinct globular domains (named domains I and II) bisected by a deep groove wherein the maltooligosaccharide ligand is bound and sequestered (5, 6). A bending motion of the hinge connecting the two domains modulates access

to and from the groove. In the sugar-free “open form” structure (Figure 1A), the two domains are far apart and the groove is easily accessible to solvents or oligosaccharides (4, 7). In contrast, in the ligand-bound “closed form” structures (Figure 1A), the form that is apparently essential for signal transduction in active transport and chemotaxis, the two domains are much closer to each other and engulf the ligand (5, 6). The groove accommodates at least four  $\alpha(1\text{--}4)$ -linked glucose units of the maltooligosaccharides in a left-handed ribbonlike conformation. In this conformation, the unbound oligosaccharides have ~3 times more accessible surface area associated with the polar atoms, mostly exocyclic OH groups, than with the small clusters of nonpolar CH bonds protruding mostly from the A-faces of the glucopyranose rings (e.g., see panels A, C, E, and G of Figure 2). The segregation of polar from nonpolar groups in the oligosaccharides is reflected by the distinct role that each domain plays in achieving near-perfect complementarity in ligand binding. Domain I provides most of the polar residues that make multiple hydrogen bonds with the oligosaccharide OH groups, whereas domain II supplies all the aromatic side chains that stack against the more nonpolar A-face of the glucopyranosides (e.g., for maltose binding, see Figure 3A) (6). In solution, the oligosaccharides bind to MBP with very rapid association rates ( $\sim 10^8 \text{ M}^{-1} \text{ s}^{-1}$ ) and  $K_d$  values in the low micromolar range (4, 6).

Given the unique system described above, we sought to identify which domain preferentially binds ligands, thereby

<sup>†</sup> This work was supported by NIH and Welch Foundation grants and the Howard Hughes Medical Institute with which F.A.Q. is an investigator.

<sup>‡</sup> Three atomic coordinate files have been deposited in the Protein Data Bank (entries 1JW4, 1JW5, and 1EZ9).

\* To whom correspondence should be addressed. E-mail: faq@bcm.tmc.edu.

<sup>§</sup> Present address: Molecular Biology Institute, University of California at Los Angeles, Los Angeles, CA 90095-1570.

<sup>1</sup> Abbreviations: ASA, accessible surface area; MBP, maltose/maltooligosaccharide-binding protein.

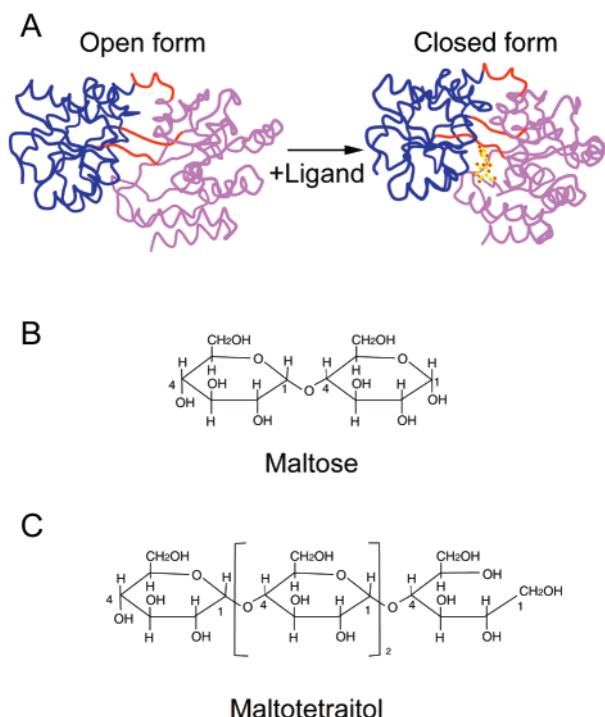


FIGURE 1: (A) Ribbon diagrams of MBP in the open sugar-free and closed maltose-bound structures. Domain I, domain II, and the hinge segments connecting the two domains are colored blue, magenta, and red, respectively. The maltose bound between the two domains is colored yellow. The structure of the open form is reported here (see Experimental Procedures), and that of the closed form is described in refs 5 and 6. (B) Maltose. (C) Maltotetraitol.

uncovering which interaction (polar or nonpolar) plays the major role in the initial process of molecular recognition and

binding. This has been facilitated by the determination of both the closed structure of MBP that had been cocrystallized with maltotetraitol (9) and the open structure also with a cocrystallized maltotetraitol reported here. Moreover, for comparison with a prior maltose-bound closed MBP structure (6), the maltose-bound open structure was determined from a preformed crystal of the unliganded open form (7) that was soaked in a maltose-containing solution. These structure analyses further shed new light on molecular recognition of carbohydrates by proteins, a fundamentally important process in myriads of biological functions, including cell–cell adhesion, inflammation, immunology, virology, fertilization, and cell development. As nonpolar and polar interactions contribute to the stability of protein structures (10, 11), the result of this analysis may have a bearing on the relative importance of each interaction as well.

## EXPERIMENTAL PROCEDURES

**Crystallization and Structure Determination.** MBP was purified and kept at 4 °C in a storage solution of 0.02% sodium azide, 10 mM 2-(*N*-morpholino)ethanesulfonic acid (pH 6.2) (5, 6). The structure of the closed form of MBP with bound cocrystallized maltotetraitol at pH 6.2 has been recently reported (9). The crystals of this form were obtained at room temperature using an almost-identical hanging drop procedure for the crystallization of the same form with bound natural maltooligosaccharide ligands (5, 6).

The procedure for obtaining cocrystals of the open form of MBP with maltotetraitol is similar to that of the closed form except that PEG 3350 was used instead of PEG 6000, the pH was set at 6.6, and crystallization was carried out in

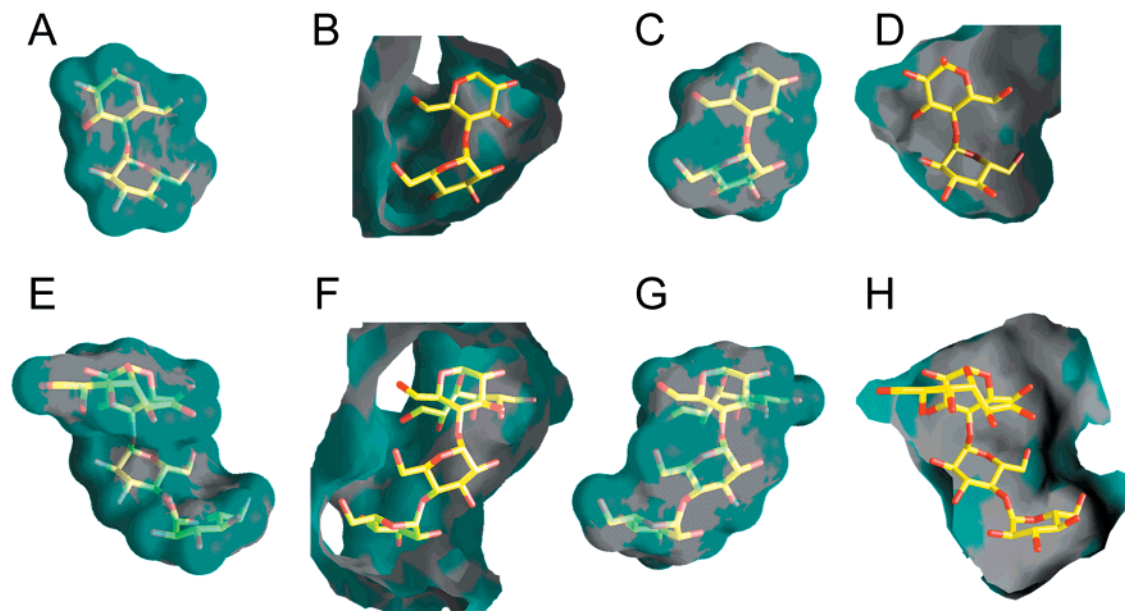


FIGURE 2: Binding interfaces of oligosaccharides and the domain I or II binding site of MBP in the closed form. Structural data for generating this set of figures are described in refs 6 and 9. Panels A, C, E, and G show, in transparent surface renditions, the accessible surfaces (polar in aqua and nonpolar in gray) of the unbound oligosaccharides. The accessible surface of the binding site contributed by each domain of MBP (panels B, D, F, and H) are rendered as opaque surface. The oligosaccharides, with the first sugar residue at the top, are drawn in stick models with the carbon and oxygen atoms colored yellow and red, respectively. The A- and B-faces of a pyranoside ring are defined as those for which the number system is clockwise and counterclockwise, respectively. (A) Predominantly polar accessible surface of the B-face of maltose. (B) Binding of maltose with its polar B-face side interfacing with the highly polar accessible surface of the site in domain I. The sugar is rotated by 180° about a vertical axis with respect to that shown in panel A. (C) Accessible surface of the A-face side of the maltose that is significantly more nonpolar than that of the B-face side shown in panel A. (D) Docking of the nonpolar A-face side of the maltose onto an almost totally nonpolar accessible surface of the domain II binding site. The sugar orientation is related to that in panel C by a 180° rotation about a vertical axis. Panels E–H are similar to panels A–D, respectively, for free and bound maltotetraitol.

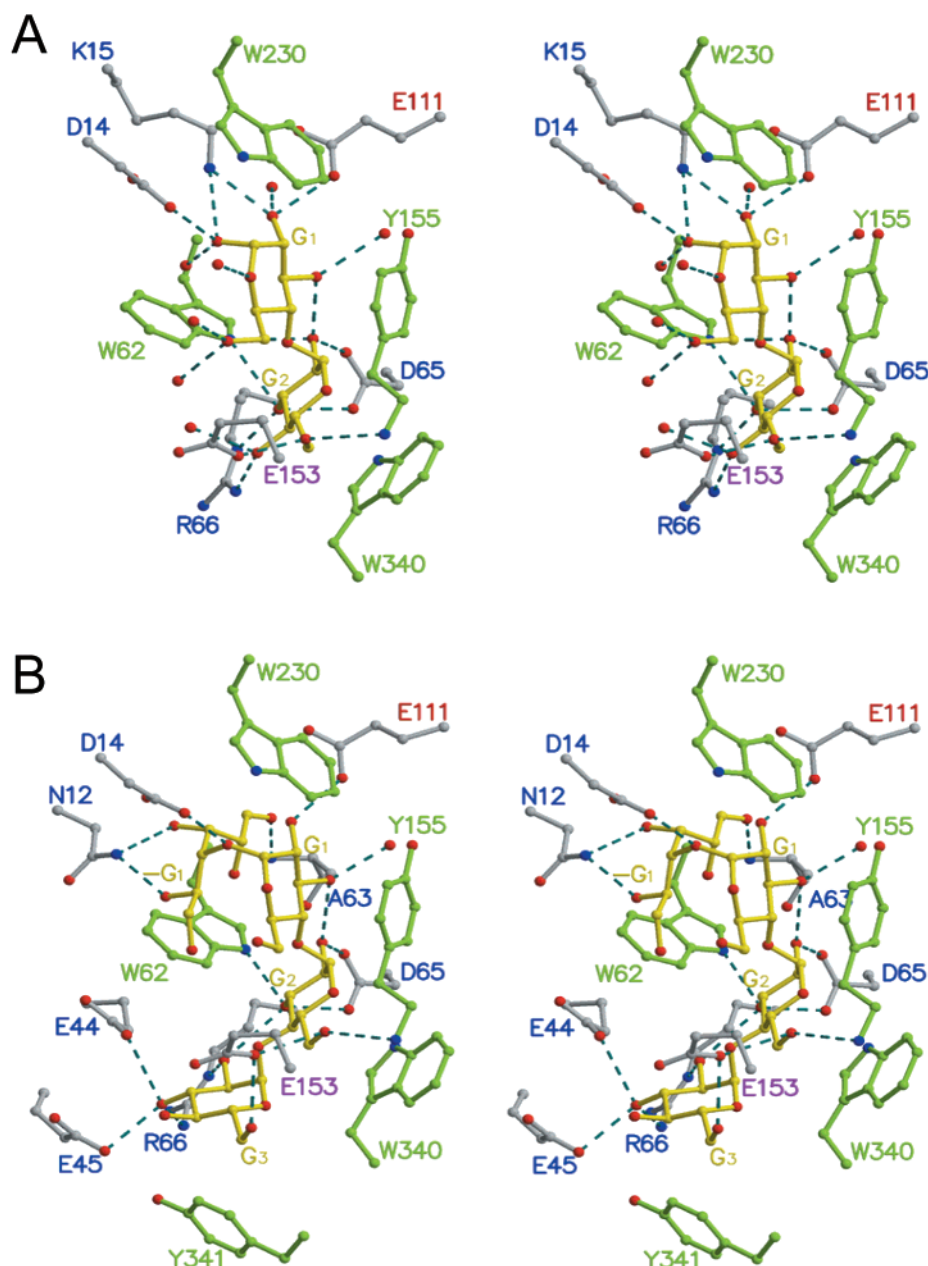


FIGURE 3: Stereoview of the interactions between maltose (A) or maltotetraitol (B) and the closed form of MBP. Structural data for generating this set of figures are described in refs 6 and 9. Blue dashed lines represent hydrogen bonds ( $\leq 3.4$  Å). The residues in domain I, domain II, and the hinge connecting the two domains are identified with the one-letter code in blue, violet, and red, respectively. The aromatic residues (colored green) originate from domain I (W62) and domain II (W230, Y155, W340, and Y341). Ordered water molecules are represented by isolated red oxygen atoms. (A) Binding of maltose with the G1 and G2 glucose residues occupying the first two (S1 and S2, respectively) of the four subsites in the binding site groove (6). All the sugar OH groups, as well as ring O5 of G1, are involved in a total of 20 hydrogen bonds, 12 with the protein, seven with ordered water molecules, and one between the G1 3-OH group and the G2 2-OH group. The water molecules hydrogen bonded to the G1 2-OH, 3-OH, and 6-OH groups and the G2 4-OH group are in turn making hydrogen bonds with five residues. (B) Binding of maltotetraitol with the open chain glucitol sugar ( $-G1$ ) followed by G1, G2, and G3 glucose residues. The  $-G1$  glucitol residue resides in a subsite ( $-S1$ ) anterior to S1. With the exceptions of four OH groups ( $-G1$  2-OH and 6-OH groups, G1 6-OH group, and G3 4-OH group), all hydroxyl groups and the oxygen of the glycosidic bond between  $-G1$  and G1 are engaged in the following number of hydrogen bonds: 16 with MBP, one with a water molecule which in turn is hydrogen bonded to MBP, and two between the G1 3-OH and G2 2-OH groups and the G2 3-OH and G3 2-OH groups.

the cold room. The initial 25  $\mu$ L drops containing 3.5 mg/mL MBP, 1 mM maltotetraitol, and 20% PEG 3350 in the storage solution (pH 6.6) were hung over wells containing 30% PEG 3350 in the same storage solution. Before the intensity data were collected, a crystal was transferred into a stabilizing storage solution of 1 mM maltotetraitol and 30% PEG 3350 (pH 6.6), and flash-cooled to  $-170$  °C. The data were collected using a MAC Science DIP2030 image plate system with double-mirror focusing optics mounted on a

Rigaku RU200 rotating anode (Cu K $\alpha$ ). The data were processed and scaled using DENZO and SCALEPACK, respectively (Table 1) (12). The structure was determined by molecular replacement using CNS (13), with the sugar-free open MBP structure (7) as the search model and reflections in the range of 9–4 Å. Consistent with the presence of two molecules in the unit cell for the *P1* space group crystal (Table 1), the rotation search gave two strong peaks (one wherein  $\varphi_1 = 239.097^\circ$ ,  $\varphi_2 = 90.000^\circ$ , and  $\varphi_3$



Table 1: Statistics of Crystallographic Data and Structure Refinement

	maltotetraitol ligand	maltose ligand	no ligand
space group	<i>P</i> 1	<i>P</i> 1	<i>P</i> 1
unit cell	<i>a</i> = 51.7 Å	<i>a</i> = 37.9 Å	<i>a</i> = 38.1 Å
dimensions	<i>b</i> = 57.9 Å	<i>b</i> = 44.6 Å	<i>b</i> = 44.6 Å
	<i>c</i> = 64.6 Å	<i>c</i> = 58.1 Å	<i>c</i> = 58.3 Å
	$\alpha$ = 89.3°	$\alpha$ = 100.6°	$\alpha$ = 99.6°
	$\beta$ = 81.8°	$\beta$ = 101.0°	$\beta$ = 101.6°
	$\gamma$ = 72.0°	$\gamma$ = 103.7°	$\gamma$ = 104.5°
<i>Z</i>	2	1	1
resolution (Å)	1.9	2.0	2.0
completeness (%)	91.9	89	87.7
redundancy	1.6	1.8	1.6
<i>R</i> <sub>sym</sub> (%)	4.1	4.2	4.3
<i>I</i> / <i>σ</i> ( <i>I</i> )	18	17	16
<i>R</i> -factor (%)	19.1	19.9	20
<i>R</i> -free (%)	23.5	25	26
no. of ordered waters	763	301	397
rmsd for bond distances (Å)	0.01	0.01	0.01
rmsd for bond angles (deg)	1.3	1.2	1.3

= 181.497° and the other wherein  $\varphi_1 = 231.294^\circ$ ,  $\varphi_2 = 95.000^\circ$ , and  $\varphi_3 = 176.954^\circ$ , both of which were 3 times greater in magnitude than the next highest peak. With the center of the first molecule fixed arbitrarily at the origin, a translation function search of the second molecule yielded one peak with the following fraction coordinates:  $x = 0.513$ ,  $y = 0$ , and  $z = 0.488$ . After an initial rigid body refinement, which lowered the *R*-factor to 39.7%, the model, together with bound water molecules and maltotetraitol, was refined to convergence at 1.9 Å resolution (Table 1). Because the two molecules (A and B) in the asymmetric unit, which are

related by slight rotation and translation, are very similar, the A molecule is used to describe the structure here. From an identical crystallization setup as described above, we also obtained a different crystal form (*P*2<sub>1</sub> space group) of the maltotetraitol-bound open form. The structure of this form (9) is virtually identical to the structure reported here.

Crystals of the sugar-free, open form of MBP were obtained as previously described (7). The crystals, which were first equilibrated in a solution of 35% PEG 20000 and 20 mM 2-(*N*-morpholino)ethanesulfonic acid (pH 6.2), were soaked for 7 days in the same solution containing 10 mM maltose and then flash-cooled to −170 °C. Diffraction data were collected as described above (Table 1). The structure of the soaked crystal was determined by direct phasing with the isomorphous structure of the sugar-free MBP (7) and refined at 2 Å resolution (Table 1). For comparison with the two ligand-bound open structures described above determined at −170 °C, we have also collected a 2 Å data set from a crystal of the open ligand-free form that was flash-cooled to an identical temperature and then used for structure refinement (Table 1).

**Accessible Surface Area Calculations.** The solvent accessible surface area (14) of protein structures (with ordered water molecules removed from the coordinates) was calculated and displayed (Figures 2 and 4 and Table 2) within the GRASP program using a probe radius of 1.4 Å and the van der Waals radius of atoms provided in the program (15). Surfaces of carbon and sulfur atoms were classified as nonpolar (hydrophobic), whereas those of oxygens and nitrogens were classified as polar (hydrophilic).

## RESULTS AND DISCUSSION

Like the normal maltooligosaccharides bound in the closed form of MBP (6), the cocrystallized maltotetraitol shows

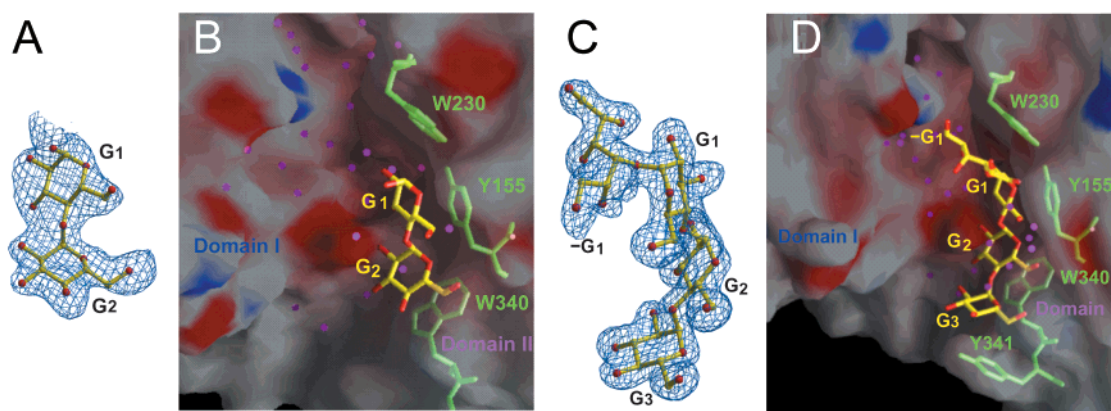


FIGURE 4: Binding of maltose and maltotetraitol to domain II of MBP in the open form. The isolated oxygen atoms in magenta represent ordered water molecules. (A) The 2 Å resolution difference electron density at the 2 $\sigma$  level of the bound maltose. (B) Electrostatic surface potential (−25*kT*, red; neutral, white; 25*kT*, blue), rendered as a transparent surface, of a region of the open binding site groove of MBP (in the same orientation as shown in Figure 1A) with maltose exclusively bound in domain II. Of the MBP–maltose hydrogen bonds shown in Figure 2A, only three are retained in the open form, two with residues (labeled in violet) in domain II (E153 OE1 and Y155 N with the G2 6-OH group) and one with a residue (blue label) in the hinge (E111 OE1 with the G1 2-OH group). The one hydrogen bond between the two glucose residues is also retained. Additionally, the G1 1-OH and 6-OH groups and the G2 4-OH group are engaged in five hydrogen bonds with ordered water molecules. The G1 3-OH and G2 2-OH groups of maltose make no hydrogen bond. (C) The 1.9 Å resolution difference electron density at the 2 $\sigma$  level of the maltotetraitol bound in one (molecule A) of the two molecules in the open structure (see Experimental Procedures). (D) Similar to panel B but with bound maltotetraitol and one additional aromatic residue (T341) from domain II contacting the sugar. Of the MBP–sugar hydrogen bonds shown in Figure 2B, only four are retained in the open form, three involving domain II residues (violet label) (E153 OE1 with the G2 6-OH and G3 6-OH groups and Y155 N with the G2 6-OH group) and one with a hinge residue (blue label) (E111 OE1 with the G1 2-OH group). These four hydrogen bonds, together with 11 others with water molecules and three between sugar units (two between glucose residues and one between the −G1 2-OH and G1 2-OH groups), leave four unpaired hydroxyl groups (−G1 5-OH and 6-OH, G1 6-OH, and G3 3-OH).

excellent complementarity with the binding site groove. Maltotetraitol, a glucitol derivative of maltotetraose (Figure 1C), binds with a  $K_d$  value ( $8\ \mu\text{M}$ ) (16) that is comparable to the values for the binding of normal maltooligosaccharides (6). In the closed structure, the maltotetraitol, which is almost totally buried (loss of 90% of the free accessible surface area), is bound by both MBP domains in a manner very similar to that observed previously for the binding of maltooligosaccharides (6). The most specific interactions between MBP and maltotetraitol are 16 hydrogen bonds (Figure 3B), of which 12 are made with the polar residue-rich domain I. Three hydrogen bonds are formed with two residues of domain II, and one hydrogen bond is made with a residue of the hinge. As expected of a mostly buried, predominantly polar ligand, all but four of the 15 OH groups of maltotetraitol are engaged in hydrogen bonding interactions, including those with the protein and one ordered water molecule and two between sugar units (Figure 3B). As six of the sugar hydroxyl groups serve as donors and acceptors simultaneously, they are engaged in stable cooperative hydrogen bonds. Ten hydrogen bonds are formed with charged side chains (Figure 3B), of which seven occur in domain I.

The maltose that is completely buried in the closed structure makes a total of 12 hydrogen bonds with MBP (Figure 3A), significantly more per sugar residue than the number of bonds to the bound maltotetraitol. Nine hydrogen bonds are formed with domain I. There are also seven hydrogen bonds with water molecules, of which four are in turn making hydrogen bonds with the protein. In contrast with the bound maltotetraitol, every hydroxyl group of the maltose is engaged in multiple hydrogen bonds with mostly charged residues. Complexes of three other active transport/chemotaxis receptors with monopyranosides exhibit very similar features of polar interactions (17–19), although the ratio of the number of hydrogen bonds per sugar hydroxyl is higher in these interactions than the ones described here. Furthermore, in all of the complexes involving the receptors (including MBP), the geometries of the hydrogen bonds are nearly ideal. The hydrogen bond distances exhibit a mean value of  $2.9\ \text{\AA}$ , with shorter distances for nearly all of those between carboxylate side chains and sugar hydroxyl groups, and the bond angles are close to  $180^\circ$ . Experimental studies of the binding of deoxy and fluoro- or chlorodeoxy sugars indicate a value of approximately  $-1.8\ \text{kcal/mol}$  for the strength of a hydrogen bond between a carboxylate and a sugar hydroxyl formed in a completely buried receptor site (20, 21). Finally, it has been previously noted of complexes of other proteins with carbohydrates that hydrogen bonds per buried surface area are more dense and a greater proportion of them involve charged groups than those observed in the protein interior (22). Taken together, the above molecular features of carbohydrate binding strongly suggest that hydrophilic or electrostatic interactions make a major contribution to the stability of protein–carbohydrate complexes (6, 22, 23). A similar major role of polar interactions has been proposed for protein–protein interactions (24, 25).

Another notable feature of the closed form of MBP with bound maltooligosaccharides (5, 6), including maltotetraitol, is the involvement of four aromatic side chains (Trp 230, Tyr 155, Trp 340, and Tyr 341) that reside exclusively in

domain II in hydrophobic interactions (Figure 3). The spiral alignment of the aromatic side chains creates a punctuated nonpolar surface that nearly matches the outer curvature (or the A-face side) of the left-handed ribbonlike oligosaccharide structure (panels D and H of Figure 2 and panel B of Figure 3). As a result, the side chains interface with the small nonpolar clusters from the A-faces of the three glucose rings of maltotetraitol (panels G and H of Figure 2 and panel B of Figure 3). For maltose binding, the first three aromatic side chains stack against the A-faces of the two glucose rings (panels C and D of Figure 2 and panel A of Figure 3). The one aromatic residue (Trp 62) in domain I that is directed toward the inner curvature of both maltose and maltotetraitol, which is more polar than the outer curvature (panels A, C, E, and G of Figure 2), makes almost no stacking interactions. Instead, it lies approximately perpendicular to the B-face of the G2 glucose unit, permitting a hydrogen bond between the Trp ring NE1H and G2 3-OH (panels A and B of Figure 3). The proximity of aromatic side chains to bound carbohydrates, as exemplified by the MBP–oligosaccharide complexes, is also a recurrent feature of carbohydrate binding to almost all of more than 50 proteins and/or enzymes with known structures (26–28). Besides the hydrophobic stacking interactions, aromatic residues have been proposed to play an additional role in carbohydrate recognition by negative selection or steric conflict of sugar epimers (26, 29).

In the open ligand-bound structures of MBP, the diffused maltose and the cocrystallized maltotetraitol were found to be associated almost exclusively with domain II (Figure 4) in a manner very similar to that with the same domain in the closed form structures (Figure 3). The nonpolar stacking interactions of the aromatic residues with the A-faces of the glucose residues and the few hydrogen bonds between domain II and the sugar OH groups observed in the closed structures are retained in the open structures (see the legend of Figure 4). The fact that the open form has now been seen in three different crystal lattices, including the structures of the sugar-free MBP (7) and the two ( $P1$  and  $P2_1$  space groups) maltotetraitol-bound proteins (described here and in ref 9), clearly demonstrates that the existence of this form is not influenced by crystal packing. Remarkably, these open structures exhibit very similar geometries, including the relative orientation and opening of the groove between the two domains (9). Moreover, with the exception of approximately three residues that undergo conformational changes upon binding of oligosaccharides longer than maltose, the region in domain I that forms part of the entire ligand-binding site groove is also very similar in both the open and closed bound structures. The geometrical feature that appears to stabilize the open form with bound maltotetraitol and the possible mechanism for the rearrangement to the closed form have been presented (9).

Determining the change in accessible surface area ( $\Delta\text{ASA}$ ) that accompanies complex formation in the closed and open forms not only further confirmed the distinct role that each domain plays in ligand binding but also revealed new features of carbohydrate recognition (Table 2). In the closed form, the two domains almost equally sequester the sugars. For example, the interactions of domains I and II with maltose bury 321 and  $384\ \text{\AA}^2$  of accessible surface area, respectively. Reflecting the highly polar nature of the ligands and the binding groove (or the binding interface), a majority ( $\sim 65\%$ )

Table 2: Changes in Accessible Surface Areas ( $\Delta$ ASAs) as a Result of the Formation of Complexes between the Receptor and Oligosaccharides<sup>a</sup>

ligand	structure form	$-\Delta$ ASA ( $\text{\AA}^2$ )					
		total		domain I with ligand		domain II with ligand	
		polar	nonpolar	polar	nonpolar	polar	nonpolar
maltose	closed	429	248	251	70	193	191
	open	266	227	34	0	204	226
maltotetraitol	closed	726	404	399	148	321	266
	open	458	386	62	16	347	373

<sup>a</sup> Calculation of solvent accessible surface area is described in Experimental Procedures. The  $\Delta$ ASA for the complex is the difference between the area of the complex and the summed surface areas for the protein and the sugar molecule separated from each other. When the loss of accessible surface area is partitioned into domains I and II, 7 and 2% of the combined total  $\Delta$ ASAs of both domains in the closed and open structures, respectively, represent the surface area of the sugar contacting both domains. Excluded from the combined total of  $\Delta$ ASAs of domains I and II with ligands is the loss of accessible surface due to the interaction between the ligand and the hinge region, which is approximately 7% of the combined total. These two factors account for the small discrepancy between this combined total and the sum of the total polar and nonpolar  $\Delta$ ASAs. The greater decrease in polar and nonpolar  $\Delta$ ASAs due to the interaction of the maltotetraitol with domain II in going from the closed structure to the open structure is attributed to an increase in the area of the interface between the glucitol unit ( $-\text{G1}$ ) and domain II in the open structure. This contributes to several polar–nonpolar contacts. The glucitol makes no hydrogen bond with the protein in the open structure.

of the total buried surface (677 and 1130  $\text{\AA}^2$  for the complexes with maltose and maltotetraitol, respectively) is polar, which encompasses mostly the hydrogen bonding interactions with domain I. Significantly more polar surface area is buried in domain I (251 and 399  $\text{\AA}^2$  for maltose and maltotetraitol, respectively) than nonpolar surface (70 and 148  $\text{\AA}^2$  for maltose and maltotetraitol, respectively). Not surprisingly, a greater proportion of the total nonpolar  $\Delta$ ASA ( $\sim 72\%$  for the complex with maltose and  $\sim 64\%$  for that with maltotetraitol) is attributed to the interactions with domain II which include the stacking interactions between the aromatic residues and the nonpolar clusters of the sugars.

In the open MBP, there is, as expected, a significantly smaller overall decrease in total buried ASAs (493 and 844  $\text{\AA}^2$  for the complexes with maltose and maltotetraitol, respectively) (Table 2). This is attributed almost entirely to a smaller amount of buried polar accessible surface since domain I no longer participates in ligand binding. In contrast, the total nonpolar  $\Delta$ ASAs for both complexes remain essentially the same as in the closed structures, confirming that most of the hydrophobic interactions occur in the aromatic residue-rich domain II.

A noteworthy finding is the substantial buried polar surface area associated with the interaction between domain II and the ligands in the open form (Table 2). Indeed, the  $-\Delta$ ASA (polar) of this interaction changes very little from the closed to the open form and is also nearly equivalent to the  $-\Delta$ ASA (nonpolar). This finding indicates that a significant fraction of the binding interface in the open form, as well as in the closed form, is noncomplementary, mostly between the polar sugar hydroxyl groups and nonpolar atoms of the aromatic side chains. More importantly, this finding further implies a smaller actual contact surface involved in purely hydrophobic interactions. It is also noteworthy that these

hydrophobic interactions enable the ligands to bind initially to domain II with rates near the diffusion limit, and thus, the hydroxyl–aromatic contacts are not detrimental to rapid binding.

Our study further indicates the presence of many ordered water molecules in the entire length of the groove between the two domains in the open form structures. The groove contains 30–40 ordered water molecules, less than half of which are lodged between domain I and the sugar-loaded site in domain II (Figure 4). These ordered water molecules help prevent voids and provide hydrogen-bonding partners to the exposed polar groups of the side chains and oligosaccharides. In the closed sugar-bound MBP structures, the entire groove contains  $\sim 15$  ordered water molecules. A favorable entropic contribution from expulsion of the water molecules in the groove that accompanies domain closure, concomitant with the formation of the hydrogen bonds between the sugar hydroxyl groups and the polar groups of domain I, should contribute to the more stable closed form that is essential for signal transduction in active transport and chemotaxis.

In conclusion, we have provided compelling experimental evidence from structural analysis for a dominant role of hydrophobic interaction in the initial binding of a protein to ligands even under conditions where the ligands have far greater potential for more specific polar interactions which would also remove polar reactant surface from bulk solvent exposure. Since the interior of a protein does not even contain the large proportion of buried hydrogen bonds described here or in other receptor–carbohydrate complexes, polar interaction is extremely unlikely to be a dominant force in the stability of protein structures.

Because aromatic residues occur almost universally in carbohydrate-binding sites of proteins, nonpolar interaction is likely to be central to ligand recognition and binding. This interaction may also prevail in the binding of cyclic sugar homologues such as inositides that are biologically important molecules for signaling and membrane trafficking. Aromatic residues need not be a prerequisite, however, as first demonstrated by the close contact of a methyl side chain of a methionine residue with a relatively small exposed nonpolar patch from the A-face of the monopyranosides bound to the L-arabinose-binding protein (17, 26, 30). The new findings presented here may have significant ramifications for understanding protein–ligand molecular recognition processes. They also provide the impetus for the effort to find conditions under which initial ligand binding could be redirected to the domain rich in polar residues.

## ACKNOWLEDGMENT

We thank W. E. Meador for technical assistance and reading of the manuscript and Prof. H. Nikaido (Department of Molecular and Cell Biology, University of California, Berkeley, CA) for kindly providing the maltotetraitol.

## REFERENCES

- Higgins, C. F. (1992) *Annu. Rev. Cell Biol.* 8, 67–113.
- Boos, W., and Licht, J. M. (1996) in *Escherichia coli and Salmonella typhimurium Cellular and Molecular Biology* (Neidhardt, F. C., Ed.) pp 1175–1209, ASM Press, Washington, DC.



3. Stock, J. B., and Surette, M. G. (1996) in *Escherichia coli and Salmonella typhimurium Cellular and Molecular Biology* (Neidhardt, F. C., Ed.) pp 1103–1129, ASM Press, Washington, DC.
4. Quioco, F. A., and Ledvina, P. S. (1996) *Mol. Microbiol.* 20, 17–25.
5. Spurlino, J. C., Lu, G. Y., and Quioco, F. A. (1991) *J. Biol. Chem.* 266, 5202–5219.
6. Quioco, F. A., Spurlino, J. C., and Rodseth, L. E. (1997) *Structure* 5, 997–1015.
7. Sharff, A. J., Rodseth, L. E., Spurlino, J. C., and Quioco, F. A. (1992) *Biochemistry* 31, 10657–10663.
8. Miller, D. M., III, Olson, J. S., Pflugrath, J. W., and Quioco, F. A. (1983) *J. Biol. Chem.* 258, 13665–13672.
9. Duan, X., Hall, J. A., Nikaido, H., and Quioco, F. A. (2001) *J. Mol. Biol.* 306, 1115–1126.
10. Dill, K. A. (1990) *Biochemistry* 29, 7133–7155.
11. Pace, C. N., Shirley, B. A., McNutt, M., and Gajiwala, K. (1996) *FASEB J.* 29, 75–83.
12. Otwinowski, Z., and Minor, W. (1997) *Methods Enzymol.* 276, 307–326.
13. Brünger, A. T., Adams, P. D., Clore, G. M., DeLano, W. L., Gros, P., Grosse-Kunstleve, R. W., Jiang, J. S., Kuszewski, J., Nilges, M., Pannu, N. S., Read, R. J., Rice, L. M., Simonson, T., and Warren, G. L. (1998) *Acta Crystallogr. D54*, 905–921.
14. Lee, B. K., and Richards, F. M. (1971) *J. Mol. Biol.* 55, 379–400.
15. Nicholls, A., Sharp, K. A., and Honig, B. (1991) *Proteins* 11, 281–296.
16. Ferenci, T., Muir, M., Lee, K. S., and Maris, D. (1986) *Biochim. Biophys. Acta* 860, 44–50.
17. Quioco, F. A., and Vyas, N. K. (1984) *Nature* 310, 381–386.
18. Mowbray, S. L., and Cole, L. B. (1992) *J. Mol. Biol.* 225, 155–175.
19. Vyas, M. N., Vyas, N. K., and Quioco, F. A. (1994) *Biochemistry* 33, 4762–4768.
20. Vermersch, P. S., Tesmer, J. J. G., and Quioco, F. A. (1992) *J. Mol. Biol.* 226, 923–929.
21. Quioco, F. A. (1993) *Biochem. Soc. Trans.* 21, 442–448.
22. Garcia-Hernandez, E., and Hernandez, A. (1999) *Protein Sci.* 8, 1075–1086.
23. Quioco, F. A. (1986) *Annu. Rev. Biochem.* 55, 287–315.
24. Horton, N., and Lewis, M. (1992) *Protein Sci.* 1, 169–181.
25. Xu, D. X., Lin, S. L., and Nussinov, R. (1997) *J. Mol. Biol.* 265, 68–84.
26. Vyas, N. K., Vyas, M. N., and Quioco, F. A. (1988) *Science* 242, 1290–1295.
27. Vyas, N. K. (1991) *Curr. Opin. Struct. Biol.* 1, 732–740.
28. Quioco, F. A., and Vyas, N. K. (1999) in *Bioorganic Chemistry: Carbohydrates* (Hecht, S. M., Ed.) pp 441–457, Oxford University Press, Oxford, England.
29. Quioco, F. A., Vyas, N. K., Sack, J. S., and Vyas, M. N. (1987) *Cold Spring Harbor Symp. Quant. Biol.* 52, 453–463.
30. Quioco, F. A., Wilson, D. K., and Vyas, N. K. (1989) *Nature* 340, 404–407.

BI015784N